# Dependence of Signal Loss on Different Positions on The Human Body in Near-field Coupling Communication

Ibuki Yokota
Kyoto Institute of Technology
Matsugasaki Sakyo-ku
Kyoto, Japan

Masaki Ishida
Kyoto Institute of Technology
Matsugasaki Sakyo-ku
Kyoto, Japan

Tomonori Nakamura
Kyoto Institute of Technology
Matsugasaki Sakyo-ku
Kyoto, Japan

Hitoshi Shimasaki
Kyoto Institute of Technology
Matsugasaki Sakyo-ku
Kyoto, Japan
shimasaki@kit.ac.jp

Yuichi Kado
Kyoto Institute of Technology
Matsugasaki Sakyo-ku
Kyoto, Japan
kado@kit.ac.jp

## ABSTRACT
Near-field coupling communication (NFCC) is a technology that uses the surface of the human body as a transmission path in the MHz band. It is necessary to assess the signal loss on the body to ensure stable NFCC links. The dependence of signal loss on different positions on the body was measured with a transmitter powered by a battery and an electrically isolated probe as a receiver. The dependence of signal loss on different poses of the body was also measured. The electric-field distributions on the body were evaluated with a high frequency structure simulator (HFSS). Results demonstrated that the signal loss is affected by both the shape and the pose of the body.

## Categories and Subject Descriptors
B.4.1 [**INPUT/OUTPUT AND DATA COMMUNICATIONS**]: Data Communications Devices – *Receivers, Transmitters.*
B.4.2 [**INPUT/OUTPUT AND DATA COMMUNICATIONS**]: Input / Output Devices -*Channels and controllers*

## General Terms
Measurement, Design, Reliability, Experimentation, Security, Human Factors, Standardization

## Keywords
Near-field coupling communication, Electrically isolated measurement, Path/Signal loss, Electrical-to-optical and optical-to-electrical conversion.


BODYNETS 2014, September 29-October 01, London, Great Britain

DOI 10.4108/icst.bodynets.2014.257017

## 1. INTRODUCTION
Wireless body area networks (WBANs) around the human body are technologies that can be utilized as convenient new applications in areas such as medical information, security, and payment systems. Such technologies have the potential to accelerate ubiquitous societies and thereby improve the quality of life. Body-channel communication (BCC), one of the WBAN technologies, has recently been garnering attention [1]. We previously proposed near-field coupling communication (NFCC), method that uses the surface of the body as a data transmission path in the MHz band by inducing a weak electric-field signal on the surface. This technology features two types of transceiver, one worn on the body (wearable TRX) and one embedded in various environments or equipment (embedded TRX) [2], and two communication types, one for communication between wearable TRXs (on-body communication) and the other between wearable and embedded TRXs (off-body communication) [3]-[4]. NFCC for off-body communication can be established only when users with the wearable TRX perform a specific action (such as touching or stepping on the electrodes of the embedded TRX) because the main characteristic of NFCC using the frequency of 6.75 MHz (i.e., below 10 MHz) is its short radial distance. We aim to establish a "touch and connect" form of communication using NFCC. One of the potential applications of our NFCC system is an entry/exit control system in a train station.

Figure.1 shows an example of a ticket gate system using NFCC in a train station. All the passengers have a wearable TRX that contains a two-way communication function. The electrodes connected to the embedded TRX are installed under the floor board of the ticket gate. The wearable and embedded TRXs mutually communicate information such as the fare and entry/exit points when a passenger steps on the embedded electrodes. This system enables passengers to pass through the gate and be charged without having to take any action such as taking or inserting a ticket. This type of gate would be user-friendly for any passenger linked up with the NFCC technology.

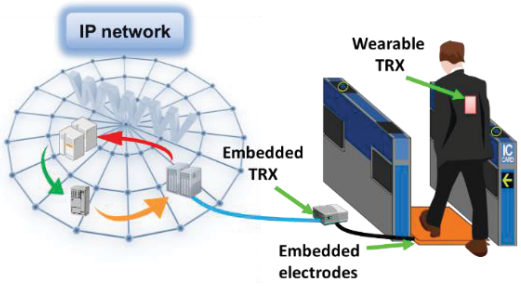


**Figure 1. Train ticket gate application.**

With NFCC, it is necessary to assess signal loss on the body in order to design a stable communication link. We have previously reported signal loss on a phantom made of gel to clarify the basic facts in NFCC [4]. However, for practical use, results using the real human body are required.

In this study, we estimated the dependence of signal loss on different positions on the human body in order to determine the best position to locate a wearable TRX. The dependence of signal loss on different poses of the body was also estimated and the electric-field distributions on a human model were evaluated with a high frequency structure simulator (FFSS). The results indicate that, to achieve a stable NFCC link, the wearable TRX should be placed around the pants pocket.

## 2. EQUIVALENT CIRCUIT

A simple signal path model for the NFCC system between wearable and embedded TRXs is outlined in Fig. 2. In this model, we regard the human body as a conductor in the 6.75 MHz frequency range used for communication, shown as a node in the figure. Capacitance $C_1$ is between the ground electrode of a wearable TRX and the body, $C_2$ is between the ground electrode of a wearable TRX and the floor ground, and $C_3$ is between the signal electrode of a wearable TRX and the body. Other capacitances that do not affect signal path are excluded in this paper. The signal loop consists of two path types, forward and return, called an up-link when the wearable TRX transmits a signal and the embedded TRX receives it and called a down-link when the embedded TRX transmits a signal and the wearable TRX receives it.

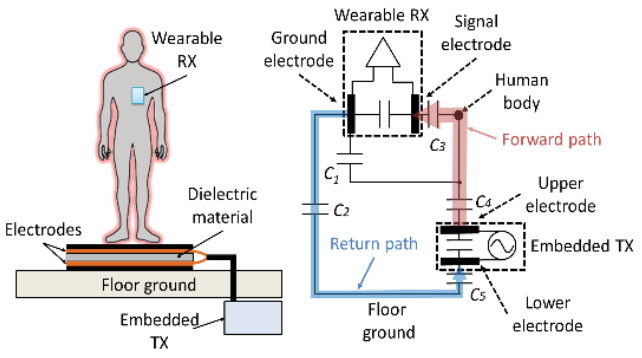


**Figure 2. Equivalent circuit and signal path models.**

## 3. MEASUREMENT SYSTEM

### 3.1 E/O and O/E Probe

We designed and fabricated a probe consisting of an electrical-to-optical (E/O) converter and an optical-to-electrical (O/E) converter to reduce the return path enhancement caused by electrically connecting the electrodes to a measurement instrument and to accurately measure signal losses [4]. A block diagram of the E/O and O/E probe is shown in Fig. 3. The electrodes are parallel copper plates the same size as those in the wearable TRX. The probe head receives the electrical signal, the E/O circuit converts the electrical signal to an optical signal, and the O/E circuit reconverts the optical signal to an electrical signal. The circuit gain of the E/O-O/E probe is 23.8 dB at 6.75 MHz.

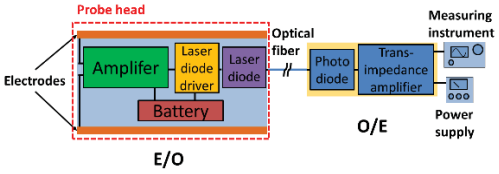


**Figure 3. Block diagram of E/O and O/E probe.**

### 3.2 Battery-Powered TX

We developed a battery-powered TX that generates a sinusoidal wave signal of about 10 $V_{p\text{-}p}$ at 6.75 MHz to reduce the return path enhancement caused by electrically connecting the electrodes to a signal generator and to accurately measure signal losses [5]. Photographs and a block diagram of the TX are shown in Fig. 4. The dimensions of the TX are 85 × 54 × 6.5 mm. The distance between the two electrodes is 6.5 mm. The signal electrode in the TX is 36.8 $cm^2$ and the ground electrode is 19.5 $cm^2$, the same as the wearable TRX.

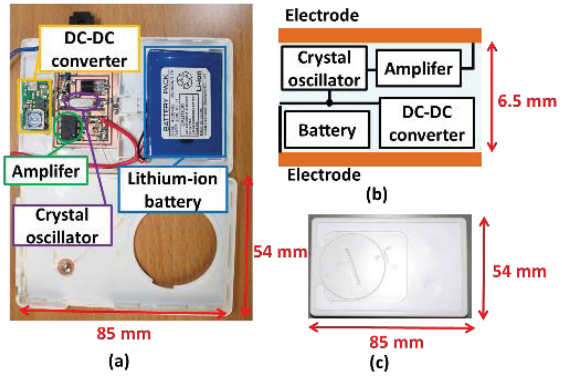


**Figure 4. (a) Photograph of battery-powered TX, (b) block diagram of battery-powered TX, and (c) photograph of proposed wearable TRX.**

### 3.3 Suit and case

We used a full-body suit for repeated measurements on the body. The full-body suit was held together with Velcro tape that was made of polyester. The probe head or battery-powered TX was placed in a polyethylene terephthalate case and attached to the suit. Photographs of the suit and the case are shown in Figs. 5 (a) and (b), respectively.

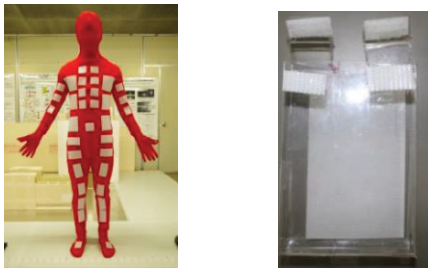

(a) (b)

**Figure 5. (a) Suit used for measurement and (b) case.**

## 4. EXPERIMENTS AND SIMULATIONS

We experimentally measured signal path loss between the wearable and embedded TRXs on a human body. The human was a 23-year-old male (height: 165 cm). We also evaluated the electric-filed distribution around the human model via the simulations.

The schematics of our experimental systems are shown in Figs. 6 (a) and (b). We measured the received voltage with the E/O-O/E probe for the down-link and the embedded electrode for the up-link as a receiver. The electrodes were connected to a measurement instrument or signal generator as a substitute for an embedded TRX and measured 350 × 350 mm. An 8-mm-thick polyethylene plate was placed between the electrodes. We used the E/O-O/E probe for the down-link and battery-powered TX for the up-link as a substitute for a wearable TRX. A 6.75 MHz frequency sinusoidal wave was transmitted with a signal generator for the down-link and battery-powered TX for the up-link. The floor ground was connected to the power source ground, which was distinguished from the earth ground [6].

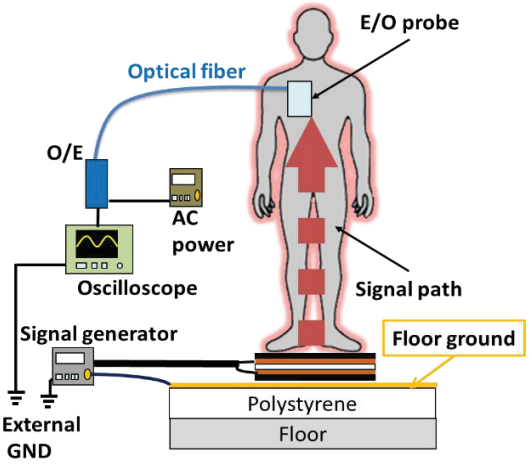


(a)

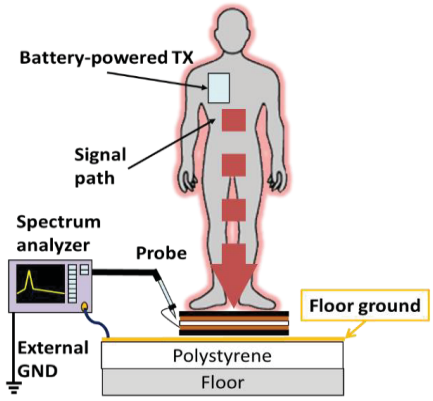


(b)

**Figure 6. Experimental systems on the human body for (a) down-link and (b) up-link.**

The boundary conditions for the simulations are summarized in Fig. 7. In these simulations, we drew the structures of a human model and the wearable and embedded TRXs with the CAD tool of the HFSS. The body structure of the human model was equivalent to that of a 30-year-old male (height: 170 cm). The body structure homogeneously had the same electrical properties, conductivity, and relative permittivity as the muscles of a human body, specifically, 0.60 S/m and 234 at 6.75 MHz [7]. The electrodes of the wearable TRX were parallel copper sheets, as shown in Fig. 7 (a). The electrodes of the embedded TRX were also parallel copper sheets, as shown in Fig. 7 (b). In Fig. 7 (c), a situation is assumed in which the body wearing the wearable TRX was standing on the embedded TRX. The wearable TRX was placed on various positions of the body. A sinusoidal wave signal of 1 $V_{p-p}$ at 6.75 MHz was generated between the electrodes of the embedded TRX for the down-link and the same signal was generated between the electrodes of the wearable TRX for the up-link.

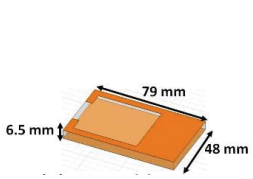


(a)

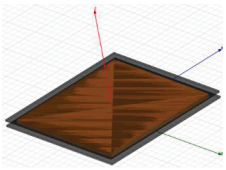

(b)

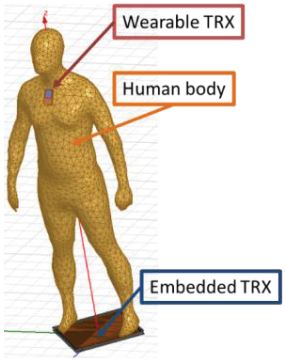


(c)

**Figure 7. Boundary conditions for simulations of (a) electrodes of wearable TRX, (b) electrodes of embedded TRX and (c) human body.**

## 5. RESULTS

We calculated signal loss on the body for the up-link and down-link, which was represented by the ratio of the received voltage to the transmission voltage defined as:

$$\text{Signal loss} = -20 \times \log\{\frac{\text{Received voltage}}{\text{Transmitted voltage}}\} \quad (1)$$

The results of signal loss on different positions on the body for the down-link and up-link are shown in Figs. 8 (a) and (b), respectively. The signal loss on the navel was the reference value. The results demonstrate that the signal losses did indeed depend on different positions on the body. Specifically, the signal losses on the torso were within ±2 dB, and the losses on the shoulder and the side of the arms were relatively high while those on the front of the arms and chest were relatively low. We assume that these differences stem from the change of capacitance $C_1$. For example, capacitance $C_1$ when the wearable TRX was on the shoulder or the side of the arms was smaller than when it was on the navel. This means that the signal path through $C_1$ decreased and the return path increased. Interestingly, the signal losses on the front of the arms or chest were bigger than those on the navel. This indicates the same thing, i.e., that the signal path through $C_1$ increased and the return path decreased. These results clearly demonstrate that the signal loss depends on the position on the body. We conclude that the wearable TRX should not be placed on the arms, since the difference between signal loss on the side of the arms and the front of the arms was approximately 9 dB.

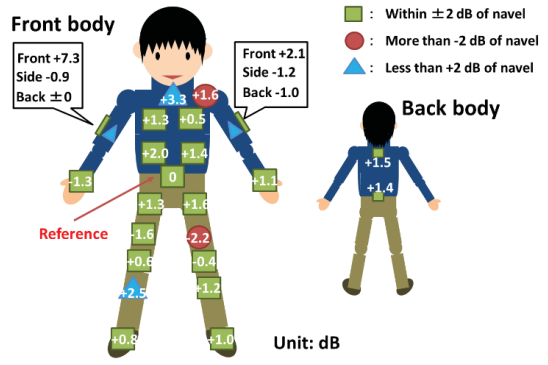


(a)

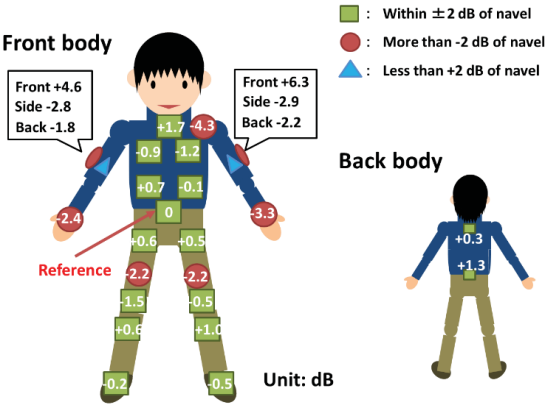


(b)

**Figure 8. Dependence of signal loss on positions on human body for (a) down-link and (b) up-link.**

We repeated this down-link experiment several times to evaluate the reproducibility error range of the signal losses on the positions. The results are shown in Figs. 9 (a), (b), and (c). The reproducibility error range of the signal loss on the torso was equal to 3 dB or less. We assume these errors were caused by the suit sagging due to the weight of the probe head. This sag decreased the capacitance $C_3$ and therefore the forward path also decreased. Interestingly, the maximum reproducibility error range of the signal loss was 6 dB. We assume this is because it was hard to place the arms and legs at the exact same position in every experiment. These results indicate that it is difficult to accurately measure the signal loss on the arms or legs by using a real body, so ideally we should use a human-shaped phantom for such measurements. However, we used a rectangular phantom in previous experiments. Additional measurements using a human-shaped phantom that has the same electrical characteristics as the body need to be done. From the above experimental results, we conclude that, to achieve stable NFCC links, one of the best positions to locate the wearable TRX is around the pants pocket.

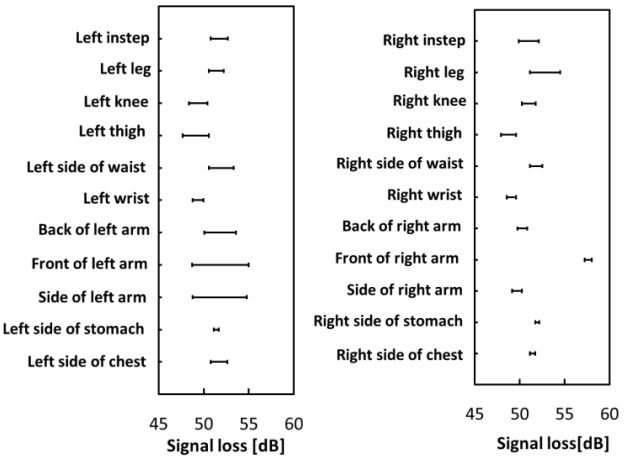


(a) (b)

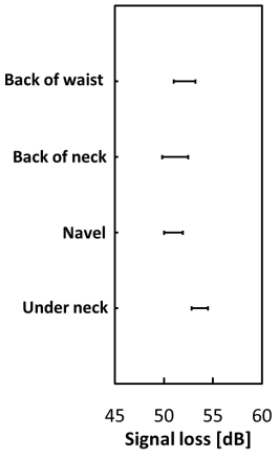


(c)

**Figure 9. Reproducibility error in measured signal loss on human body.**

Photographs of the poses used to evaluate the dependence of signal loss on positions of the body are shown in Fig. 10. The probe head for the up-link and battery-powered TX for the down-link were fixed on the left side of the chest. The poses included raising a hand, extending the hands forward, opening the arms, and standing on one leg.

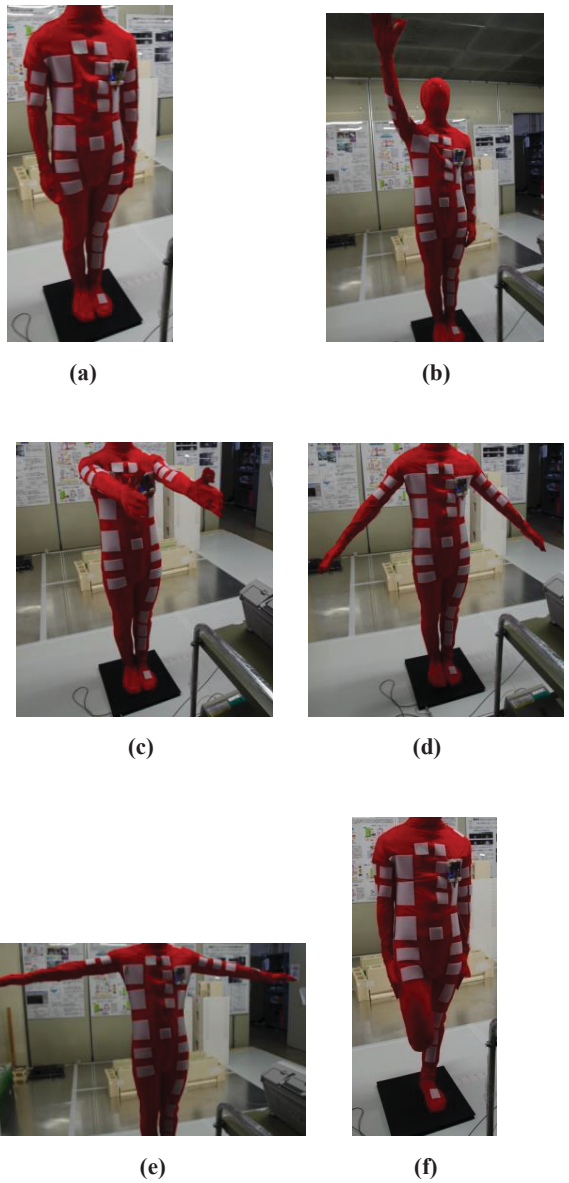

**Figure 10. Poses for measuring signal loss: (a) standing upright, (b) raising a hand, (c) extending hands forward, (d) opening arms (90°), (e) opening arms (45°), (f) standing on one leg.**

The results of our experiments are summarized in Table 1. The signal loss on the standing upright pose was the reference value. The signal loss on the pose for extending the hands forward was lower than that for standing upright by approximately 13 dB for the down-link and 16 dB for the up-link. When the hands were extended forward, the probe head for the down-link and battery-powered TX for the up-link was enclosed by the arms, which increased the capacitance $C_1$. This means that the signal path through $C_1$ increased and the return path decreased. We therefore recommend that the positions of the body be considered when designing link budget components, transmission power, and minimum receiver sensitivity.

**Table 1. Dependence of the signal loss on type of poses.**

| Pose | | Down-link [dB] | Up-link [dB] |
|---|---|---|---|
| Standing upright | | 0 | 0 |
| Raising a hand | Right hand | 0.32 | 0.79 |
| | Left hand | 3.24 | 4.01 |
| Extending hands forward | | 12.82 | 15.71 |
| Opening arms | 45° | 1.19 | 1.56 |
| | 90° | 1.50 | 2.81 |
| Standing on one leg | Left leg | 1.64 | 2.09 |
| | Right leg | 1.41 | 2.06 |

When the probe head for the up-link and battery-powered TX for the down-link was fixed around the pelvic area, the signal loss on the poses barely changed. We therefore recommend placing the wearable TRX around the pants pocket to achieve a stable NFCC link.

Figure 11 shows the simulated electric-field distributions around the human model for the down-link.

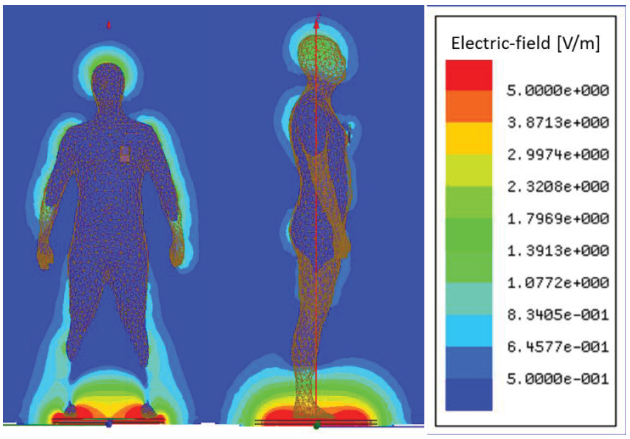


**Figure 11. Electric-field distributions for down-link.**

These results indicate that the intensity of the electric-field did not depend on the distance between the embedded TX and wearable RX. The electric-field around the edges of the body -e.g.,

the head, arms, and shoulders- was stronger than that around other areas, while the electric-field on concave portions of the body - e.g., the chest, armpits, and around the neck area- was weaker than that around the edges of the body. These characteristics in the simulation results are similar to those in the experimental results. However, in the simulation results, the electric-field on the torso was stronger than that on the navel, and in the experimental results, the signal loss on the torso was stronger than that on the navel. These differences stem from the fact that the surface of the torso in the simulations was not flat compared to that in the experiments. We found that the concave and convex portions of the body affect the quality of the NFCC links.

Figure 12 shows the electric-field vectors around the body when the wearable TX was placed on the side, front and back of the arm for the up-link. The number of electric-field vectors in a direction of the air in the case of the side of the arm in Fig. 12 (a) is larger than that in the case of the front and back of the arm in Fig.12 (b) and (c). This means that the electric coupling between the signal electrode of the wearable TX and the floor GND in the case of the side of the arm was stronger than that in the case of the front and back of the arm. The electric coupling increased the capacitance $C_2$ and made the return path increase in the case of the side of the arm. In contrast, the electric coupling between the ground electrode of the wearable TX and the body increased the capacitance $C_1$ and made the return path decrease in the case of the front and back of the arm. These dependences of the simulation results correspond equally to those of the experimental results, demonstrating that capacitances $C_1$ and $C_2$ change depending on the position of the wearable TRX on the human body.

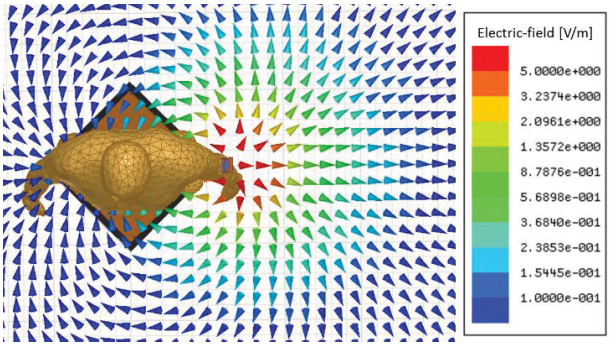


(a)

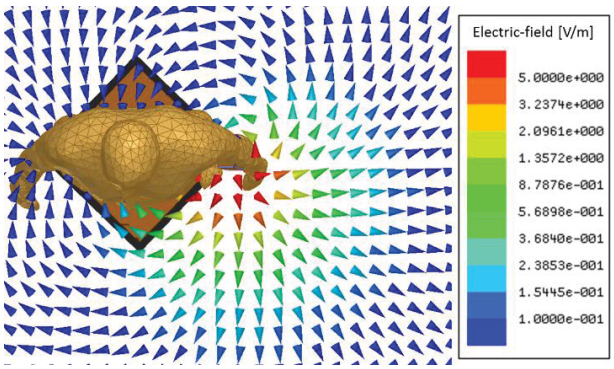


(b)

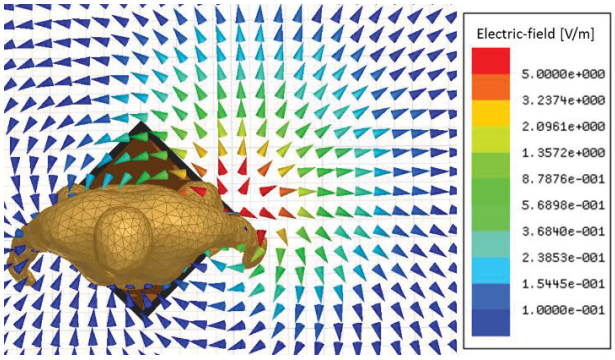


(c)

**Figure 12. Electric-field vectors when the wearable TX is placed on the (a) side, (b) front and (c) back of the arm.**

## 6. CONCLUSION

We proposed communication using NFCC for the MHz band between wearable and embedded TRXs on the human body. We estimated the signal loss on different positions on the body to design link budget components, transmitter power, and minimum receiver sensitivity. Simulation and experimental results showed that the signal loss does indeed depend on both the positions and the poses of the body. The difference between the signal loss on the side of the arms and the front of the arms was approximately 9 dB. When the wearable TRX was placed on the left side of the chest, the signal loss on the pose for extending the hands forward was lower than that for standing upright by approximately 13 dB for the down-link and 16 dB for the up-link. These differences adversely affected the quality of the NFCC links. We consequently determined that, to achieve stable communication links for NFCC applications, the best position for the wearable TRX is around the pants pocket. We evaluated the electric-field intensity around the body with an HFSS and confirmed that the electric-field distribution depends on the shape of the body and the position of the wearable TRX. We conclude that the signal loss on the body is dependent on the surface shape and the actual poses of the body.

## 7. ACKNOWLEDGMENTS

Part of this work was supported by a Grant-in-Aid for Scientific Research (A) 23246073 from the Ministry of Education, Culture, Sports, Science and Technology of Japan.

## 8. REFERENCES

[1] T. G. Zimmerman, “Personal Area Networks: Near-field intrabody communication”, *IBM Syst. J.* ,Vol. 35, no. 3/4, pp. 609 - 617, 1996.

[2] Y. Kado, T. Kobase, T. Yanagawa, T. Kusunoki, M. Takahashi, R. Nagai, O. Hiromitsu, A. Hataya, H. Shimasaki, and M. Shinagawa : “Human-Area Networking Technology Based on Near-Field Coupling Transceiver”, *2012 IEEE Radio & Wireless Sym. (RWS 2012),* pp. 119 - 122, 2012.

[3] M. Ishida, T. Nakamura, M. Nozawa, N. Watanabe, Y. Kado, and M. Shinagawa, ”MHz-Band RF Signal Propagation Characteristics on Human Body for Intra-body communication”, *IEEE International Instrumentation and*

*Measurement Technology Conference 2014*, pp. 797 - 801, 2014

[4] M. Nozawa, T. Nakamura, H. Simasaki, Y. Kado and M. Shinagawa, “Signal Measurement System Using Electrically Isolated Probe for MHz-Band Near-Field Coupling Communication”, *IEEE International Instrumentation and Measurement Technology Conference 2013*, pp. 37 - 40, 2013.

M. Ishida, T. Nakamura, M. Nozawa, N. Watanabe, H. Shimasaki, Y. Kado, and M. Shinagawa, ”Signal Propagation Characteristics between Transceivers on Human Body for Mhz-Band Near-field Coupling Communication”, *8th international Conference on body area networks*, pp. 453 - 456, 2013